

A Model of Variability in Brain Stimulation Evoked Responses

Stefan M. Goetz and Angel V. Peterchev, *Member, IEEE*

Abstract—The input-output (IO) curve of cortical neuron populations is a key measure of neural excitability and is related to other response measures including the motor threshold which is widely used for individualization of neurostimulation techniques, such as transcranial magnetic stimulation (TMS). The IO curve parameters provide biomarkers for changes in the state of the target neural population that could result from neurostimulation, pharmacological interventions, or neurological and psychiatric conditions. Conventional analyses of IO data assume a sigmoidal shape with additive Gaussian scattering that allows simple regression modeling. However, careful study of the IO curve characteristics reveals that simple additive noise does not account for the observed IO variability. We propose a consistent model that adds a second source of intrinsic variability on the input side of the IO response. We develop an appropriate mathematical method for calibrating this new nonlinear model. Finally, the modeling framework is applied to a representative IO data set. With this modeling approach, previously inexplicable stochastic behavior becomes obvious. This work could lead to improved algorithms for estimation of various excitability parameters including established measures such as the motor threshold and the IO slope, as well as novel measures relating to the variability characteristics of the IO response that could provide additional insight into the state of the targeted neural population.

I. INTRODUCTION

A key measure for characterizing the dose–response of brain stimulation methods, such as transcranial magnetic stimulation (TMS), is the input–output (IO) curve which describes the relationship of the peripheral motor response to the cortical stimulus strength [1]–[9]. Various other measures and procedures are derived from this relationship, e.g., the motor threshold [10]. The IO curve is an important detection measure, for example, for analyzing changes of cortical excitability [4], [9]. Furthermore, the motor threshold is commonly used for individualizing TMS in research and clinical applications to ensure effective and safe stimulus intensity [11].

However, single motor responses are highly fluctuating due to neural variability, and so is the whole IO curve [12]–[17]. Therefore, regression techniques, commonly least-squares fitting, are used for extracting characteristics from the variable IO data points (see, e.g., [1], [3], [8]).

The cortical stimulus–response behavior is still not well understood and the sources of variability are not known, although many possible mechanisms have been analyzed,

including summation due to the electromyographic (EMG) electrode size [18]. Nevertheless, observations of IO data coupled with basic understanding of the behavior of neural ensembles could suggest appropriate modeling approaches. The stochastic properties of the response are important for choosing a method for a regression or other description of individual characteristics. Incorrect incorporation of ‘errors’ in a regression could lead to inaccurate parameter estimation.

Statistical analysis of motor responses has shown that they exhibit most likely a multiplicative variability [19] which leads to a more consistent definition of the IO curve as the logarithm of the peak-to-peak voltage amplitude as a function of the stimulation strength. This approach reduces markedly the unaccountable variability and is adopted in our modeling method. However, even with logarithmic normalization of the IO data, the distribution of responses varies significantly depending on the stimulus amplitude (i.e., the position along the IO curve). Unfortunately, this fact is often ignored, resulting in potentially inaccurate IO parameter estimation.

To address these limitations, we propose a model of characterizing IO curve data that—in addition to the additive error assumed in standard curve-regression techniques—incorporates variability of the neural excitability before the dominant nonlinearity of the system. In other words, we consider stochastic error not only at the output of the neural circuit but also at the input.

A clear mathematical treatment of this concept of neural response including both input and output variability could provide neurophysiologic and biophysical insights that are otherwise obscured. The mathematical formulation is similar to a measurement problem where the input and output measurements of a system are noisy [20], although the underlying problem here is different: In brain stimulation, the stimulus amplitude is accurately known, but the sensitivity or excitability of the stimulated neurons incorporates a stochastic term. In contrast to most engineering problems where distinct error sources at the input and output can be analyzed by separate readout, there is no independent access to the different variability mechanisms in the brain.

We propose a relatively simple but mathematically consistent framework for solving the problem and use several advantages of the special case of IO curves that lead to a robust parameter estimation approach for neurophysiology.

II. APPROACH

A. PROBLEM ANALYSIS

The structure of the problem is depicted in Fig. 1. The stimulus with strength x depolarizes the target neuron population. The degree of neural activation resulting from the

S. M. Goetz is with Department of Psychiatry & Behavioral Sciences, Duke University, Durham, NC 27710, USA and Technische Universität München, 80333 Munich, Germany; stefan.goetz@duke.edu.

A. V. Peterchev is with the Departments of Psychiatry & Behavioral Sciences, Biomedical Engineering, and Electrical & Computer Engineering, Duke University, Durham, NC 27710, USA angel.peterchev@duke.edu.

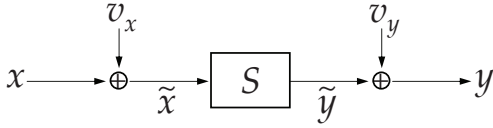


Fig. 1. Block diagram of an input-output (IO) response model. Variable x is the stimulus amplitude, S is the sigmoidal neural population recruitment characteristic, and y is the response defined as the logarithm of the peak-to-peak electromyographic (EMG) amplitude. Independent stochastic variables v_x and v_y with their density functions g_{v_x} and g_{v_y} model variability before and after the sigmoidal nonlinearity, respectively. Variables \tilde{x} and \tilde{y} are the input and output of the sigmoid characteristic module S , respectively.

stimulus is perturbed by a stochastic component v_x . This variability may be due to short-term fluctuations of the excitability of a neuron which leads to a changing threshold. Input fluctuations may also result from variability in the coil position to which TMS is very sensitive. The sigmoid transfer characteristics S represents the neural population recruitment. The variability v_y at the output of S is the conventional noise source assumed in IO modeling, which may result from fluctuations in the spinal pathway and the two synapses leading to the muscle cells, as well as EMG amplifier noise. Statistical information about the stochastic terms v_x and v_y is unknown and has to be estimated from IO data.

B. MATHEMATICAL FRAMEWORK

For linear systems, a number of methods can be applied for the analysis, such as total least squares regression. In the case of nonlinear systems, on the other hand, methods are more problem-specific.

We present an approach that models y stochastically in distribution with all dependencies on the model parameters and other influences in forward direction. Since the available amount of data for an IO curve is usually small, in our example we replace all unknown components in the explicit form of this general analytic formulation in a second step with parametric representations. The parametric model provides a full conditional distribution for a pair of corresponding stimulus and response (x, y) that can be trained subsequently with standard methods using the available measurements.

In general, this system is not uniquely solvable without exact knowledge of the factors of influence; the interplay of two stochastic influences leads to an inverse problem. The strong nonlinearity of the IO curves, however, allows a relatively stable separation of both, as shown below. Due to the changing derivative along the sigmoid, point estimators and Bayesian methods exhibit a unique minimum of their objective if the spread of both stochastic processes is not so high as to ‘wash out’ the maxima and minima of the sigmoid’s derivative.

For a fixed stimulation amplitude x , the density function $f_{\tilde{x}}(\tilde{x})$ of the effective activation level \tilde{x} is trivially $g_{v_x}(\tilde{x} - x)$ where g_{v_x} is the distribution of the variability source v_x . The

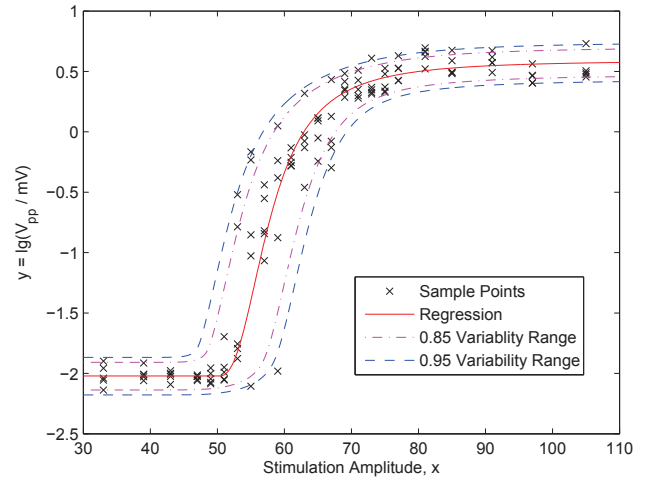


Fig. 2. Measured TMS IO curve (black crosses) and regression curve with 0.85 and 0.95 variability ranges. The y-axis shows the log-transformed peak-to-peak EMG response, V_{pp} , to a TMS stimulus with amplitude given on the x-axis. The stimulation amplitude is specified as percentage of the peak capacitor voltage of a Magstim Rapid device; a value of 100 corresponds to 1.65 kV.

nonlinearity transforms the distribution according to

$$|f_{\tilde{y}|x}(S(\tilde{x})) dS(\tilde{x})| = |f_{\tilde{x}}(\tilde{x}) d\tilde{x}| \quad (1)$$

$$= |g_{v_x}(\tilde{x} - x) d\tilde{x}| \quad (2)$$

where $dS = dS(\tilde{x}) = \frac{dS}{d\tilde{x}} d\tilde{x}$ denotes a classical differential. The second variability source v_y interplays with the distribution of \tilde{y}

$$\begin{aligned} |f_{y|x}(y) dS(\tilde{x})| &= \left| \int_{\mathbb{R}} g_{v_y}(\chi) \cdot f_{\tilde{y}|x}(y - \chi) dS d\chi \right| \quad (3) \\ &= \int_{\mathbb{R}} g_{v_y}(\chi) \cdot g_{v_x}(S^{-1}(y - \chi) - x) |d\tilde{x}| d\chi \end{aligned}$$

Expression (3) provides a full analytic description of the output y in distribution dependent on the input x and the other factors of influence (S , g_{v_x} , g_{v_y}). With this basis, the model can be combined with an appropriate estimation method. As the samples in IO curves are usually sparse due to the required long inter-stimulus intervals and limited practical length of recording sessions, in this paper we describe a parametric estimation approach. However, this modeling framework can also be the basis for a nonparametric regression.

Since this is the first time that motor cortex IO curves are modeled with the representation in Fig. 1, empirical information that could act as a prior for a Bayesian approach is not available. In addition, we do not perform a large dataset analysis in this paper; consequently, we could not benefit from statistical properties of the posterior distribution. Therefore, we keep the example simple and use a standard likelihood point estimator [21].

For parametrized distributions g_{v_x} and g_{v_y} with respective parameter vectors \mathbf{p}_1 , as well as \mathbf{p}_2 and the sigmoidal function S with parameters \mathbf{p}_3 , the likelihood is

$$L = p(\mathbf{y}|\mathbf{x}, \mathbf{p}) = \prod_i f_y(y_i|x_i, \mathbf{p}). \quad (4)$$

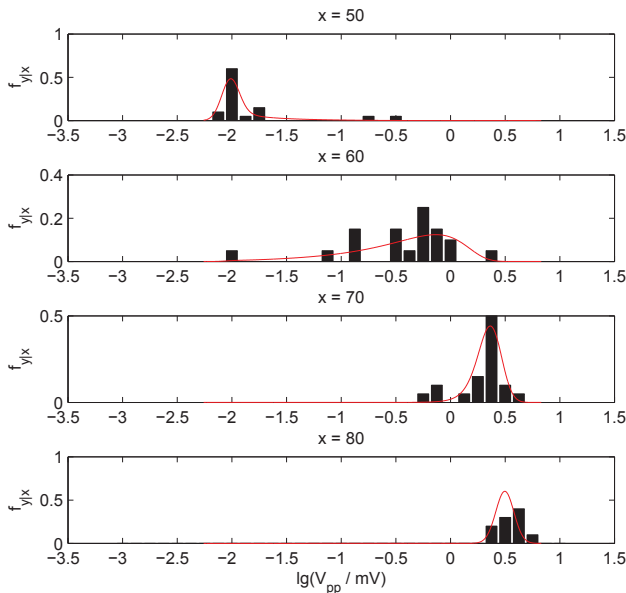


Fig. 3. Comparison of the distributions of the total variability in y at different levels of x . The black bars represent the measured values of the IO curve. The estimated density function in y (red) shows clearly the known phenomenon that the distribution has varying spread and skewness along the IO curve.

The parameters and all single IO samples (x_i, y_i) are compiled to single vectors, $\mathbf{p} = (\mathbf{p}_1, \mathbf{p}_2, \mathbf{p}_3)$, $\mathbf{x} = (x_i)_{i \in 1, \dots, m}$, and $\mathbf{y} = (y_i)_{i \in 1, \dots, m}$, respectively, where m is the number of samples. The parameter estimation is performed in the standard way by maximizing the locally convex logarithm of the likelihood.

III. EXAMPLE

We demonstrate the performance of the modeling and estimation method described above with a representative example. An IO curve of a healthy volunteer (female, age: 28) was obtained from an existing dataset [22]. In this recording, a standard figure-8 TMS coil was used in combination with a monophasic near-rectangular pulse source with a pulse width of $60 \mu\text{s}$. The peak-to-peak EMG responses, V_{pp} , were log-transformed.

The IO recording comprised only 120 sample points. Therefore, we chose a low-dimensional parametrization of the density functions in order to avoid a high-variance problem: Both variability sources are modeled as normally distributed, with the standard deviations treated as degrees of freedom. In the case of v_y , this represents a multiplicative log-normal distribution in the raw (not log-transformed) data. Knowledge of the standard deviations is not required, as they will be estimated.

The sigmoidal curve S was modeled by a Hill-type function

$$S(\bar{x}) = a + \frac{b-a}{1 + \frac{c}{(\bar{x}-e)^d}} \quad (5)$$

with parameter vector $\mathbf{p}_3 = (a, b, c, d, e)$.

The integral in Equation (3) has no analytic solution for the functions chosen here and is therefore evaluated

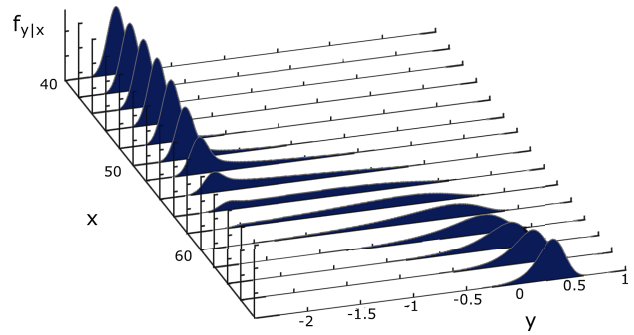


Fig. 4. The output distribution $f_{y|x}$ (axis of ordinates) at different input amplitudes x (axis of abscissae) for the most likely parameter set from the example IO curve. The distribution shape changes dramatically depending on the value of x .

numerically. The maximum in the log-likelihood was detected with an ordinary Nelder-Mead iteration [23]. The resulting regression curve and the 0.95 and 0.85 probability ranges extracted from the estimated distributions are plotted in Fig. 2. The variability ranges are extracted from the estimated model distribution $f_{y|x}$. The most likely parameter vector for this IO curve is $(a, b, c, d, e, \sigma_x, \sigma_y) = (-2.02, 0.592, 143, 2.44, 50.2, 3.04, 0.0793)$, where σ_x and σ_y are the standard deviations of the variability sources v_x and v_y , respectively. For comparison, a standard regression with variability contributed solely by v_y leads to a notably different parameter set, $(a, b, c, d, e, \sigma_x, \sigma_y) = (-2.03, 0.687, 77.8, 1.98, 48.3, 0, 0.271)$.

Figure 3 compares the distortion of the output distribution at various stimulation amplitudes x between the measurement and the model. Fig. 4 depicts the estimated distributions in more detail. The model indeed predicts the skewed, shifting distributions seen in the experimental data.

As seen in Figures 2–4, in the transition region between the IO curve plateaus, the distribution of the measured data in y for a given x is highly skewed, but the skewness shifts: on the left side of the midpoint it is skewed towards higher values, whereas on the right side it is skewed towards lower values. Considering a traditional framework with v_y as the sole variability mechanism, the accumulation points on the regression curve are challenged by outliers resulting from the skewed distributions. Without considering v_x in the regression, the y -variability is overrated and the slope is underestimated due to the apparent outliers resulting from the skewed and variable output distributions. The misestimation of the slope accumulates errors in properties that are derived from the curve. For example, the motor threshold is systematically underestimated in comparison with a local median-based definition. Furthermore the problem is unnecessarily heteroscedastic; although this is rarely taken into consideration when choosing an appropriate regression method.

On the other hand, considering our model with both v_x and v_y variability sources, the behavior of the output distribution becomes easily explainable by a normally distributed v_x transformed by the nonlinearity S . The input-side stochastic source, v_x , dominates the variability in the transition between

the saturation levels (the ‘slope region’ of the IO curve), while the output-side stochastic source, v_y , dominates the variability in the saturation regions.

Finally, due to the dominating role of v_x in the transition region of the IO curve, a regression of the inverse function (x in dependence of y) with a standard least-squares regression and assumed variability on the x -side only would be a much better approach for the transition region if the full model presented here cannot be used for some reason. This approach would reduce the underestimation of the slope in that domain.

IV. Conclusions

The proposed model reduces the unaccountable variability in IO curves to a greater extent than existing models by incorporating a stochastic component that acts directly on the excitability of the activation site. This stochastic behavior at the neural system input appears at the output after being transformed by the strong sigmoid nonlinearity characteristic of the IO curve. We believe that this model is not just a descriptive artifice to fit the data, but could also provide insight into the structure of the system under study.

The stochastic input component has not been recognized previously even in detailed studies with sophisticated experimental methods (see, e.g., [15]). One reason may be that many analyses were performed at single, isolated stimulation amplitudes which obscures the different response distributions at various stimulation levels. In some studies, data at different stimulation levels that should have been treated separately due to their distinct distributions were even combined in the analysis. In addition, the fact that the TMS stimulator output can be very accurately controlled may have resulted in the misconception that the input is stable without considering inherent neural sources of variability.

This paper focused on defining a consistent model and a mathematical framework that can be used to calibrate the model. To further demonstrate the validity and utility of the model, it should be used on IO data from a sufficient subject pool representing a cross section of the general population. The proposed modeling framework could benefit the formulation of various procedures, methods, and tools for analyzing data, detecting neuromodulatory effects, and determining individual response thresholds in brain stimulation.

ACKNOWLEDGEMENTS

We thank Dr. K. Choudhury for discussions on the inter-sample variability in TMS motor evoked potentials and the anonymous reviewers for their suggestions.

REFERENCES

[1] J.B. Pitcher, K.M. Ogston, and T.S. Miles. Age and sex differences in human motor cortex input-output characteristics. *Journal of Physiology*, vol. 546, no. 2, pp. 605–613, 2003.

[2] C. Möller, N. Arai, J. Lücke, and U. Ziemann. Hysteresis effects on the input-output curve of motor evoked potentials. *Clinical Neurophysiology*, vol. 120, pp. 1003–1008, 2009.

[3] A.A. van Kuijk, L.C. Anker, J.W. Pasman, J.C.M. Hendriks, G. van Elswijk, A.C.H. Geurts. Stimulus-response characteristics of motor evoked potentials and silent periods in proximal and distal upper-extremity muscles. *Journal of Electromyography and Kinesiology*, vol. 19, pp. 574–583, 2009.

[4] E. Hoyader, A. Degardin, F. Cassim, P. Bocquillon, P. Derambure, and H. Devanne. The effects of low- and high-frequency repetitive TMS on the input/output properties of the human corticospinal pathway. *Experimental Brain Research*, vol. 187, pp. 207–217, 2008.

[5] E.M. Wassermann. Variation in the response to transcranial magnetic brain stimulation in the general population. *Clinical Neurophysiology*, vol. 113, pp. 1165–1171, 2002.

[6] B. Boroojerdi, F. Battaglia, W. Muehlbacher, and L.G. Cohen. Mechanisms influencing stimulus-response properties of the human corticospinal system. *Clinical Neurophysiology*, vol. 112, pp. 931–937, 2001.

[7] L. Niehaus, B.-U. Meyer, T. Weyh. Influence of pulse configuration and direction of coil current on excitatory effects of magnetic motor cortex and nerve stimulation. *Clinical Neurophysiology*, vol. 111, no. 1, pp. 75–80, 2000.

[8] H. Devanne, B.A. Lavoie, and C. Capaday. Input-output properties and gain changes in the human corticospinal pathway. *Experimental Brain Research*, vol. 114, pp. 329–338, 1997.

[9] M.C. Ridding, J.C. Rothwell. Stimulus/response curves as a method of measuring motor cortical excitability in man. *Electroencephalography and Clinical Neurophysiology*, vol. 105, pp. 340–344, 1997.

[10] P.M. Rossini *et al.* Non-invasive electrical and magnetic stimulation of the brain, spinal cord and roots: basic principles and procedures for routine clinical application. Report of an IFCN committee. *Electroencephalography and Clinical Neurophysiology*, vol. 91, pp. 79–92, 1994.

[11] S. Rossi, *et al.* Safety, ethical considerations, and application guidelines for the use of transcranial magnetic stimulation in clinical practice and research. *Clinical Neurophysiology*, vol. 120, no. 12, pp. 2008–2039, 2009.

[12] P. Pasqualetti, F. Ferreri. Amplitude values of motor evoked potentials: statistical properties and neurophysiological implications. *Clinical Neurophysiology Supplement*, vol. 122, S44–S45, 2011.

[13] K.R. Choudhury, L. Boyle, M. Burke, W. Lombard, S. Ryan, B. McNamara. Intra subject variation and correlation of motor potentials evoked by transcranial magnetic stimulation. *Irish Journal of Medical Science*, vol. 180, no. 4, pp. 873–880, 2011.

[14] N.H. Jung, I. Delvendahl, N.G. Kuhnke, D. Hauschke, S. Stolle, and V. Mall. Navigated transcranial magnetic stimulation does not decrease the variability of motor-evoked potentials. *Brain Stimulation*, vol. 3, pp. 87–94, 2010.

[15] K.M. Rösler, D.M. Roth, and M.R. Magistris. Trial-to-trial size variability of motor-evoked potentials. A study using the triple stimulation technique. *Experimental Brain Research*, vol. 187, pp. 51–59, 2008.

[16] D. Burke, R. Hicks, J. Stephen, I. Woodforth, and M. Crawford. Trial-to-trial variability of corticospinal volleys in human subjects. *Electroencephalography and Clinical Neurophysiology*, vol. 97, pp. 231–237, 1995.

[17] L. Kiers, D. Cros, K.H. Chiappa, and J. Fang. Variability of motor potentials evoked by transcranial magnetic stimulation. *Electroencephalography and Clinical Neurophysiology*, vol. 89, pp. 415–423, 1993.

[18] R.J.W. Dunneworld, W. van der Kamp, A.M. van den Brink, M.S. Reegt, and G. van Dijk. Influence of electrode site and size on variability of magnetic evoked potentials. *Muscle & Nerve*, vol. 21, no. 12, 1779–1782.

[19] J.F. Nielsen. Logarithmic distribution of amplitudes of compound muscle action potentials evoked by transcranial magnetic stimulation. *Journal of Clinical Neurophysiology*, vol. 13, no. 5, pp. 423–434.

[20] L.A. Stefanski. Measurement error models. *Journal of the American Statistical Association*, vol. 95, no. 452, pp. 1353–1358.

[21] R.A. Fisher. On the mathematical foundations of theoretical statistics. *Philosophical Transactions of the Royal Society of London A*, vol. 222, pp. 309–368, 1922.

[22] A.V. Peterchev, G.G. Westin, B. Luber, and S.H. Lisanby. Corticospinal response characterization with controllable pulse parameter transcranial magnetic stimulation (cTMS). *Clinical Neurophysiology Supplement*, vol. 122, pp. S191, 2011.

[23] J.A. Nelder, R. Mead. A simplex method for function minimization. *The Computer Journal*, vol. 7, no. 4, pp. 308–313, 1965.